Proceedings of the
44th IEEE Conference on Decision and Control, and
the European Control Conference 2005
Seville, Spain, December 12-15, 2005

MMAE Terrain Reference Navigation for Underwater Vehicles using Eigen Analysis

P. Oliveira*
Instituto Superior Técnico and Instituto de Sistemas e Robótica
Torre Norte, 8º andar, 1096-001 Lisboa, Portugal
pjcro@isr.ist.utl.pt

***Abstract*— The integration of a feature based positioning sensor, rooted on Principal Component Analysis, with a Multi-Model Adaptive Estimator for Terrain Reference Navigation of Underwater Vehicles is proposed and discussed in detail. Resorting to a nonlinear Lyapunov transformation, the synthesis and analysis of each of the nonlinear multirate $\mathcal{H}_2$ estimators is presented with overall guaranteed stability and optimal performance over equilibrium trajectories. Results from Monte Carlo simulation techniques to assess the performance of both the proposed feature based positioning sensor and estimation tools are included.**

***Index Terms*— Navigation Systems, Time-varying Systems, MMAE, Kalman Filters, Robot Navigation.**

I. Introduction

The design of navigation systems for underwater vehicles (UVs) relying on data from the sensor package installed onboard, without resorting to external systems, is a challenging problem [10]. Due to the strong attenuation experienced by electromagnetic waves in the water, commonly used positioning systems (GPS, LASER, RADAR,...) are not available. The navigation system accuracy continuously degrades along time due to unmodeled dynamics, time-varying phenomena, and the noise present in the measurements of the sensors installed onboard, leading to poor performance on a number of important long range missions. To overcome this limitation external acoustic positioning systems have been proposed in the past [18] and successfully integrated in navigation systems for underwater applications [1], [19]. However, tedious deployment and demanding calibration procedures of the positioning systems strongly constrain the mission scenarios and ultimately the use of Underwater Vehicles.

In the case where the missions take place in areas where detailed bathymetric data are available, one alternative has been exploited in the past: the terrain information can be used as an aiding positioning sensor to bound the error estimates on the navigation systems leading to the so called Terrain Based or Terrain Aided Navigation Systems. Applications on air [3], [7], land [4] and underwater applications [9], [17] were reported in the last decades.

*Work supported by the Portuguese FCT POSI Programme under Framework QCA III and in the scope of project MAYA-Sub of the AdI.

The most commonly used synthesis technique to address the terrain based navigation design problem has been extended Kalman Filtering [7], [17]. Correlation techniques [3], [12] and particle filters [9], [16] have also been proposed, requiring a high computational burden. Several of these authors however provide examples on instability and severe performance degradation of the proposed solutions, precluding their use in general.

This paper tries to endow the underwater robotics community with tools for terrain based navigation but departs considerably from the previous approaches. The integration of a feature based positioning sensor, rooted on optimal processing techniques of random signals, namely Principal Component Analysis (PCA) [11], [8], with a Multi-Model Adaptive Estimator (MMAE) is proposed.

The paper is organized as follows: in section II the sensor package installed onboard is described and the underlying design model is introduced. Section III reviews the background on the Karhunen-Loève transform, basis for the principal component analysis of stochastic signals. The approach for the bathymetric data decomposition is detailed and its performance is briefly characterized. In section IV a MMAE estimator based on a bank of linear Kalman filters is proposed and some properties are presented. In section V the overall performance is assessed, resorting to a series of Monte Carlo tests of a simulated model of an UV in a synthesized terrain. Finally, some conclusions are drawn in section VI.

II. Sensor package and design model

A. Notation

Let $\{\mathcal{I}\}$ be an inertial reference frame located at mean sea level in the pre-specified mission scenario with North, East, and Down axes, and let $\{\mathcal{B}\}$ denote a body-fixed frame that moves with the UV, as depicted in fig. 1. The following notation is required:

$\mathbf{p}$ $:=[x\ y\ z]^T$ - position of the origin of $\{B\}$ in $\{\mathcal{I}\}$;
$\underset{\mathcal{B}}{(}{}^{\mathcal{I}}\mathbf{v}_{\mathcal{B}})$ - linear velocity of the origin of $\{\mathcal{B}\}$ in $\{\mathcal{I}\}$, expressed in $\{\mathcal{B}\}$, i.e. body-fixed linear velocity;
$\boldsymbol{\lambda}$ $:= [\phi\ \theta\ \psi]^T$ - vector of roll, pitch, and yaw angles;
$\underset{\mathcal{B}}{(}{}^{\mathcal{I}}\omega_{\mathcal{B}})$ - angular velocity of $\{\mathcal{B}\}$ relative to $\{\mathcal{I}\}$, expressed in $\{\mathcal{B}\}$, i.e. body-fixed angular velocity.

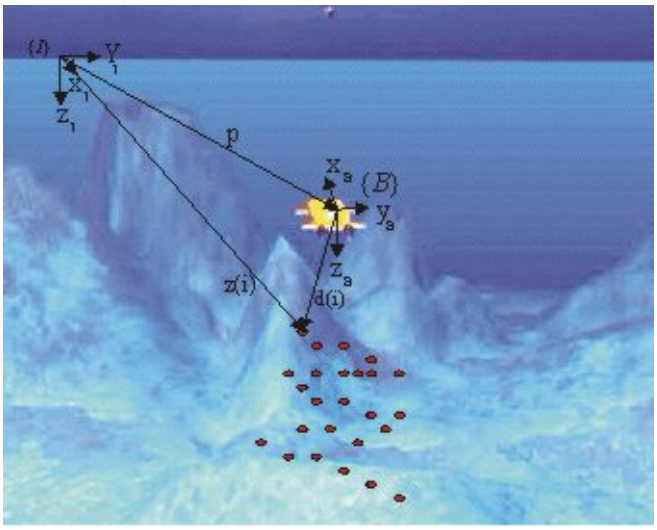

Fig. 1. UV inertial and local coordinate frames. Mechanical scanning sonar range measurements

Given two frames $\{\mathcal{A}\}$ and $\{\mathcal{B}\}$, ${}^{\mathcal{A}}_{\mathcal{B}}\mathcal{R}$ denotes the rotation matrix from $\{\mathcal{B}\}$ to $\{\mathcal{A}\}$. In particular, ${}^{\mathcal{I}}_{\mathcal{B}}\mathcal{R}(\boldsymbol{\lambda})$ is the rotation matrix from $\{\mathcal{B}\}$ to $\{\mathcal{I}\}$, parameterized locally by $\boldsymbol{\lambda}$. Since $\mathcal{R}$ is a rotation matrix, it satisfies $\mathcal{R}^T = \mathcal{R}^{-1}$ that is, $\mathcal{R}^T\mathcal{R} = I$.

B. Sensor package and data geo-referencing

Consider an UV equipped with an Attitude and Heading Reference System (AHRS) providing measurements on the attitude $\boldsymbol{\lambda}$ and on the angular velocities in body frame ${}^{\mathcal{B}}({}^{\mathcal{I}}\omega_{\mathcal{B}})$. Two rotation matrices $\mathcal{R}_Z(\psi)$ (or $\mathcal{R}_\psi$ in compact form) and $\mathcal{R}_{\theta,\phi} = \mathcal{R}_Y(\theta)\mathcal{R}_X(\phi)$ will be used, verifying ${}^{\mathcal{I}}_{\mathcal{B}}\mathcal{R}(\boldsymbol{\lambda}) = \mathcal{R}_\psi\mathcal{R}_{\theta,\phi}$. To complement the information on position, a Doppler velocity log will be installed onboard the UV, providing measurements of ${}^{\mathcal{B}}({}^{\mathcal{I}}\mathbf{v}_{\mathcal{B}})$. The body fixed velocity is expressed in the horizontal plane, using $\mathbf{v}_H = \mathcal{R}(\theta,\phi)^{\mathcal{B}}({}^{\mathcal{I}}\mathbf{v}_{\mathcal{B}})$, i.e. corrected with the attitude information in $\mathcal{R}(\theta,\phi)$, and will be an input to the design model, as detailed next. A depth cell will also be considered to provide measurements on the vertical.

A sonar ranging sensor is required to provide measurements for the PCA based positioning system, described later. Among the several types available, a mechanical scanning sonar, with a scan bearing angle ϵ, will be considered. See fig. 1 in detail, where the seafloor points sensed in consecutive ranging measurements - $z(i)$ - are depicted in red. Assuming, without loss of generality, that the sonar is installed pointing down at the origin of the reference frame $\mathcal{B}$ and the scanning angle lies in the transversal plane (containing the (y_B, z_B) axes), the i^{th} range measurement $d(i)$ can be georeferenced in the inertial reference frame $\mathcal{I}$ using the relation

$$z(i) = \mathbf{p} + {}^{\mathcal{I}}_{\mathcal{B}}\mathcal{R}(\boldsymbol{\lambda})\mathcal{R}_X(\epsilon)[0\ \ 0\ \ d(i)]^T, \tag{1}$$

where $\mathcal{R}_X(\epsilon)$ is the rotation matrix from the instantaneous sonar bearing to the UV reference frame $\mathcal{B}$. It is important to remark that no support from external systems/devices will be required.

C. Design model

The underlying design model $\mathcal{G}$ that plays a central role in the design of the estimator, depicted as part of the block diagram on fig. 3, is based on a simplified discrete time version of the UV kinematics and has the realization

$$\Sigma_{\mathcal{G}} = \left\{ \begin{array}{rcl} \mathbf{p}(k+1) & = & \mathbf{p}(k) + h\mathcal{R}_\psi(k)(\mathbf{v}_H(k) + \mathbf{b}(k)) + \eta_p \\ \mathbf{b}(k+1) & = & \mathbf{b}(k) + \mathcal{R}^T_\psi(k)\eta_b \end{array} \right. \tag{2}$$

where h is the sampling period, k describes in compact form the time instant $t_k = kh$ for $k = 0, 1, \ldots, T$ (the final mission time), $\mathbf{b}$ captures the bias terms due to velocity sensor installation and calibration mismatches, assumed constant or slowly varying, and η_p and η_b are auxiliary noise inputs to be used in the stochastic $\mathcal{H}_2$ synthesis problem addressed later.

III. Principal Component Analysis

Considering all linear transformations, the Karhunen-Loève (KL) transform allows for the optimal approximation to a stochastic signal, in the least squares sense. Furthermore, it is a well known signal expansion technique with uncorrelated coefficients for dimensionality reduction. These features make the KL transform interesting for many signal processing applications such as data compression, image and voice processing, data mining, exploratory data analysis, pattern recognition and time series prediction [11], [8].

A. PCA background

Consider a set of M stochastic signals $\mathbf{x}_i \in \mathcal{R}^N, i = 1, \ldots, M$, each represented as a column vector, with mean $\mathbf{m}_x = 1/M \sum_{i=1}^{M} \mathbf{x}_i$. The purpose of the KL transform is to find an orthogonal basis to decompose a stochastic signal $\mathbf{x}$, from the same original space, to be computed as $\mathbf{x} = \mathbf{U}\mathbf{v} + \mathbf{m}_x$, where the vector $\mathbf{v} \in \mathcal{R}^N$ is the projection of $\mathbf{x}$ in the basis, i.e., $\mathbf{v} = \mathbf{U}^T(\mathbf{x} - \mathbf{m}_x)$. The matrix $\mathbf{U} = [\mathbf{u}_1\, \mathbf{u}_2 \ldots \mathbf{u}_N]$ should be composed by the N orthogonal column vectors of the basis, verifying the eigenvalue problem

$$\mathbf{R}_{xx}\mathbf{u}_j = \lambda_j \mathbf{u}_j, \ \ j = 1, ..., N, \tag{3}$$

where $\mathbf{R}_{xx}$ is the covariance matrix, computed from the set of M experiments using

$$\mathbf{R}_{xx} = \frac{1}{M-1} \sum_{i=1}^{M} (\mathbf{x}_i - \mathbf{m}_x)(\mathbf{x}_i - \mathbf{m}_x)^T. \tag{4}$$

Assuming that the eigenvalues are ordered, i.e. $\lambda_1 \geq \lambda_2 \geq \cdots \geq \lambda_N$, the choice of the first $n << N$ principal components, leads to an approximation to the stochastic signals given by the ratio on the covariances associated with the components, i.e. $\sum_n \lambda_n / \sum_N \lambda_N$. In many applications, where stochastic multidimensional signals are the key to overcome

the problem at hand, this approximation can constitute a large dimensional reduction and thus a computational complexity reduction. The advantages of PCA are threefold: i) it is an optimal (in terms of mean squared error) linear scheme for compressing a set of high dimensional vectors into a set of lower dimensional vectors; ii) the model parameters can be computed directly from the data (by diagonalizing the ensemble covariance); iii) given the model parameters, projection into and from the bases are computationally inexpensive operations $\mathcal{O}(nN)$.

B. PCA based Positioning System

Assume a mission scenario where bathymetric data are available and that a terrain based navigation system should be designed. The steps to implemented a PCA based positioning sensor using this bathymetric data will be outlined.

Prior to the mission, the bathymetric data of the area under consideration should be partitioned in *mosaics* with fixed dimensions N_x by N_y. After reorganizing this two-dimensional data in vector form, e.g. stacking the columns, a set of M stochastic signals $\mathbf{x}_i \in \mathcal{R}^N$, $N = N_x N_y$, results. The number of signals M to be considered depends on the mission scenario and on the *mosaic* overlapping. The KL transform can be computed, using (3) and (4), the eigenvalues must be ordered, and the number n of the principal components to be used should be selected, according with the required level of approximation.

The following data should be recorded for latter use:

i) the data ensemble mean $\mathbf{m}_x$;

ii) the matrix transformation with n eigenvectors $\mathbf{U}_n = [\mathbf{u}_1 \ \ldots \ \mathbf{u}_n]$;

iii) the projection on the selected basis of all the *mosaics*, computed using $\mathbf{v}_i = \mathbf{U}_n^T(x_i - \mathbf{m}_x), i = 1, \ldots, M$;

iv) the coordinates of the center of the *mosaics*, $(x_i, y_i), \ i = 1, \ldots, M$.

During the mission, at the time instants $t_k = Lk$, with L being a positive integer, the geo-referenced range measurements from the present *mosaic*, are packed and will constitute the input signal $\mathbf{x}$ to the PCA positioning system. The following tasks should be performed:

A) compute the projection of the signal $\mathbf{x}$ into the basis, using $\mathbf{v} = \mathbf{U}_n^T(\mathbf{x} - \mathbf{m}_x)$;

B) given an estimate on the actual horizontal coordinates of the UV position $\hat{x}$ and $\hat{y}$, provided by the navigation system, search on a given neighborhood δ the *mosaic* that verifies

$$\forall_i \|[\hat{x} \ \hat{y}]^T - [x_i \ y_i]^T\|_2 < \delta, \ r_{PCA} = \min_i \ \|\mathbf{v} - \mathbf{v}_i\|_2; \quad (5)$$

C) given the *mosaic* i that is the closest to the present input, its center coordinates (x_i, y_i) will be selected as the x_m and y_m measurements.

The relation between r_{PCA} and the positioning sensor error covariance $\mathbf{R}$ (observation noise) to be used in the $\mathcal{H}_2$ estimation problem

$$\mathbf{R} = 2\,\mathbf{f^2}\,\mathbf{r_{PCA}}, \quad (6)$$

is nonlinear and space-varying and was the subject of a detailed study reported inn [15]. Note that the bathymetric data based PCA positioning system described above, can be straightforward extended to use multidimensional geophysical data that can be measured with other sensors installed onboard UVs such as magnetometers and gradiometers [10].

C. PCA Positioning Sensor Stochastic Characterization

A series of Monte Carlo tests were performed to characterize the PCA positioning sensor [15]. A summary on the impact of a number of relevant parameters is enumerated next.

Number of Principal Components - the increase on the number of components n increases the covariance accuracy explained (according to the ratio $\sum_n \lambda_n / \sum_N \lambda_N$) [11];

Number of Mosaics - In the case where the neighborhood $\delta \rightarrow \infty$ in (5), as considered in this study, the performance of the overall PCA positioning system degrades with the number of mosaics, due to the increase on the number of elements to be searched. In real applications, a careful choice of this parameter can improve the PCA performance, given an estimate on the position, as depicted in fig. 4;

Percentage of Points Scanned in a Mosaic - Due to the velocity of propagation of sound in the water, only a fraction of the total *mosaic* area can be scanned with a sonar. A graceful degradation on the performance is confirmed from the results, along any vertical line on the left of figure 2;

Terrain Bandwidth - This parameter is of utmost importance on the performance of the PCA positioning system, confirmed by the results depicted in Fig. 2. A multi-model adaptive estimator will be considered next to tackle the nonlinear relation in $\mathbf{f}$;

Mosaic Dimension - The mosaic dimension represents a compromise: small mosaic sizes increase the accuracy of the PCA positioning system, with an increase on the total number of mosaics. Large mosaic sizes diminish the accuracy and augments the correlation stored in each mosaic requiring an increase on the number of components

The results obtained reinforce the usefulness of the proposed method as a basic positioning sensor, allowing the design of bounded accuracy underwater guidance, control, and navigation systems. However, due to the nonlinear characteristics of the positioning system proposed, an adaptation method is central to accommodate the spatial variability on the mission scenario, as described in the next section.

IV. Nonlinear estimator design and analysis

The navigation system is required to provide non-biased estimates $\hat{\mathbf{p}}$ and ${}^{\mathcal{I}}\hat{\mathbf{v}}_{\mathcal{B}}$ of the position and velocity of the body

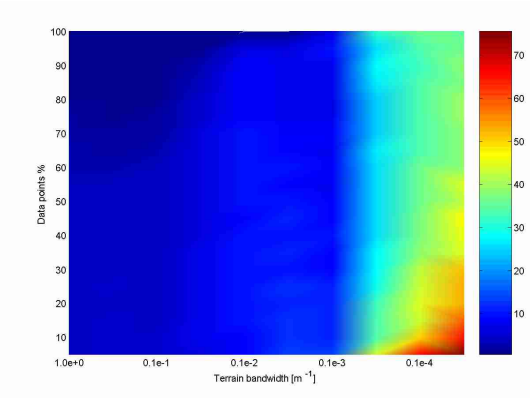

Fig. 2. Covariance relation $\mathbf{f}$ in (6), for variations on the percentage of scanned points in the mosaic versus terrain bandwidth

fixed frame $\{\mathcal{B}\}$ relative to the inertial frame $\{\mathcal{I}\}$, respectively. A classical multi-model adaptive estimator (MMAE) will be used [2], based on a bank of K Kalman filters, resorting to a common nonlinear Lyapunov transformation.

A. Nonlinear estimator design

Based on the measurements from the set of sensors installed on board and on the underlying design model, derived from the kinematic relations with realization $\mathcal{G}$ in (2), the i^{th}, $i = 1, \ldots, K$ estimator consisting of a Kalman filter will be detailed next and the overall architecture will be presented later in this section. First, some algebraic relations will be outlined, a nonlinear transformation will be introduced and applied when the UVs are describing trimming trajectories, i.e. equilibrium trajectories, see [5] for details.

On the horizontal plane the rotation of the UV admits the first order discrete time approximation $\psi(k+1) = \psi(k) + h\omega_z(k)$, where ω_z is the z component of the projection of the angular velocity in body axis to the horizontal plane, i.e. $[\omega_x \;\; \omega_y \;\; \omega_z]^T = {}^{\mathcal{I}}_{\mathcal{B}}\mathcal{R}(\boldsymbol{\lambda})^{\mathcal{B}}({}^{\mathcal{I}}\omega_{\mathcal{B}})$. Moreover, $\mathcal{R}_\psi(k+1) = \mathcal{R}_\psi(k)\mathcal{R}_Z(h\omega_z(k)) = \mathcal{R}_Z(h\omega_z(k))\mathcal{R}_\psi(k)$.

Lemma 4.1: [14] Let $\mathbf{T}(k) \in \mathcal{R}^{6\times 6}$ be a nonlinear time varying Lyapunov transformation, common to the MMAE bank of estimators to be used, parameterized by $\psi(k)$

$$\mathbf{T}(k) = \begin{bmatrix} I_{3\times 3} & 0_{3\times 3} \\ 0_{3\times 3} & \mathcal{R}_\psi(k) \end{bmatrix},$$

verifying $\mathbf{T}^{-1}(k) = \mathbf{T}^T(k)$, $\|\mathbf{T}(k)\|_2 \leq 1$, and $\|\mathbf{T}(k)\|_\infty \leq 1$.

Lemma 4.2: [14] Each estimator associated with the UV kinematics, with realization in $\mathcal{G}$, is linear and time invariant over any trimming trajectory, using the transformation $\mathbf{z_i}(k) = \mathbf{T}(k)[\mathbf{p_i}^T(k)\; \mathbf{b_i}^T(k)]^T$, introduced above.

Proof: See [14] for details. ■

Remark that the resulting dynamics will be used on the $\mathcal{H}_2$ estimator synthesis problem, where $\eta_\mathbf{i} = [\eta_{p_\mathbf{i}}^T \; \eta_{b_\mathbf{i}}^T]^T$ is zero mean white noise with uncorrelated covariance

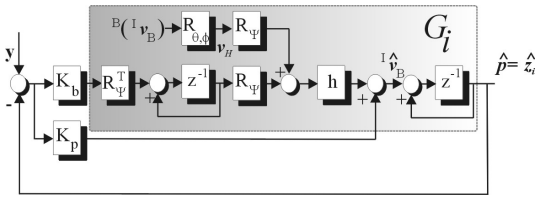

Fig. 3. Block diagram of each nonlinear estimator proposed (with some abuse of notation)

$E[\eta_\mathbf{i}(k)\eta_\mathbf{i}^T(k)] = \mathbf{Q_i}(k)$. The multirate problem will be solved resorting to the usual nonlinear recursions for the Kalman filter:

$$\begin{array}{rcl} \hat{\mathbf{z}}_\mathbf{i}^-(k+1) & = & \overline{\mathbf{A}}(k)\hat{\mathbf{z}}_\mathbf{i}^+(k) \quad + \quad \overline{\mathbf{B}}_1(k)\mathbf{v}_H(k) \\ \mathbf{P}_\mathbf{i}^-(k+1) & = & \overline{\mathbf{A}}(k)\mathbf{P}_\mathbf{i}^+(k)\overline{\mathbf{A}}^T(k) \quad + \quad \mathbf{Q_i}(k) \\ & & \text{for } i = 1, \ldots, K \end{array} \tag{7}$$

where $\hat{\mathbf{z}}_\mathbf{i}^-(k+1)$ is the predicted state variable estimate and $\mathbf{P}_\mathbf{i}^-(k+1)$ is the covariance of the prediction estimation error, respectively, for the i^{th} estimator.

In the time instants multiple of L, the PCA positioning system, described in subsection III-B, and the depth cell provide measurements $\mathbf{y} = [x_m \;\; y_m \;\; z_m]^T$, with covariance $\mathbf{R_i}(k) = diag(f\, r_{PCA}^{1/2}, f\, r_{PCA}^{1/2}, r_m)$. The Kalman filter state and error covariance updates, $\hat{\mathbf{z}}^+(k)$ and $P^+(k)$, respectively, can be obtained according with

$$\begin{array}{rcl} \hat{\mathbf{z}}_\mathbf{i}^+(k) & = & \hat{\mathbf{z}}_\mathbf{i}^-(k) + \mathbf{K_i}(k)(y - \overline{\mathbf{C}}\hat{\mathbf{z}}_\mathbf{i}^-(k)) \\ \mathbf{P}_\mathbf{i}^+(k) & = & \mathbf{P}_\mathbf{i}^-(k) - \mathbf{P}_\mathbf{i}^-(k)\overline{\mathbf{C}}^T \\ (\overline{\mathbf{C}}\mathbf{P}_\mathbf{i}^-(k)\overline{\mathbf{C}}^T + \mathbf{R_i}(k))^{-1}\overline{\mathbf{C}}^T\mathbf{P}_\mathbf{i}^-(k) & & \end{array} \tag{8}$$

where $\mathbf{K_i}(k) = \mathbf{P}_\mathbf{i}^-(k)\overline{\mathbf{C}}^T(\overline{\mathbf{C}}\mathbf{P}_\mathbf{i}^-(k)\overline{\mathbf{C}}^T + \mathbf{R_i}(k))^{-1} = [\mathbf{K}_{p_\mathbf{i}}^T \; \mathbf{K}_{b_\mathbf{i}}^T]^T$ is the Kalman gain, with two diagonal blocks. For the time instants $mod(k, L) \neq 0$ $\mathbf{P}_\mathbf{i}^+(k) = \mathbf{P}_\mathbf{i}^-(k)$ and $\hat{\mathbf{z}}_\mathbf{i}^+(k) = \hat{\mathbf{z}}_\mathbf{i}^-(k)$. The resulting estimator is represented in fig. 3, with some abuse of notation.

Under the assumption of homogeneous space properties, note that the covariances in both x and y directions of the initial error covariance $\mathbf{P}_\mathbf{i}^-(0)$, the state noise covariance $\mathbf{Q_i}$ for all estimators, and the observation covariances from the PCA positioning system are identical. The observation covariance $\mathbf{R_i}$ will be considered different for each model, as detailed next, and the hypothesis conditional probability will be computed by the MMAE estimator.

It is important to remark that is this case the probability density functions are symmetric and under a rotation they are preserved (the level curves are circles). This fact supports the use of a linear Kalman filter for the nonlinear system and explains the fact that over any trimming trajectory the evolution of the estimate covariances are correctly described, which is clearly not true in the general case.

Interestingly, the proposed structure is a Complementary Filter [13]. The low-pass characteristics from the PCA position measurement to the position estimate are of utmost importance to reject the high frequency noise due to finite space

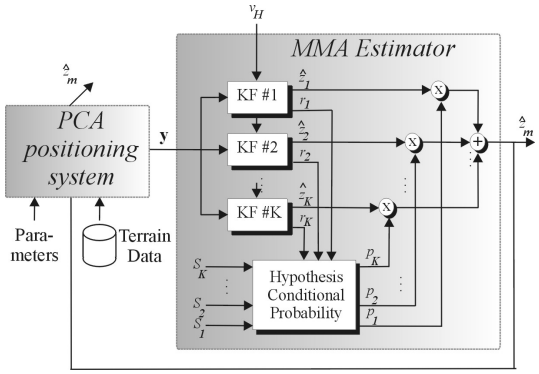

Fig. 4. Multi-model adaptive estimator architecture

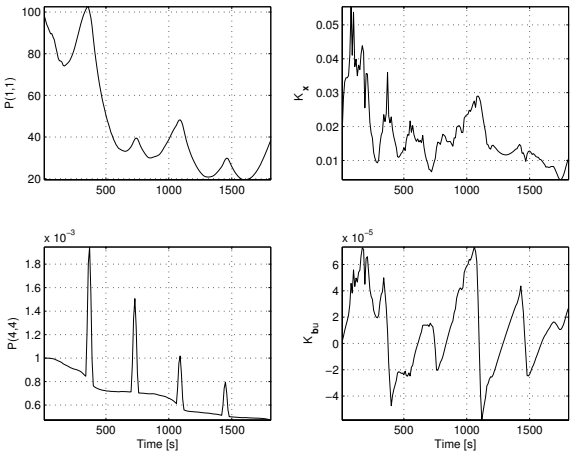

Fig. 5. Estimator covariances for horizontal position axes ($x = y$) and horizontal bias, upper and lower left pictures, respectively. Position and bias estimator gains, upper and lower right pictures

resolution imposed by the dimensions of the *mosaics* chosen. The bias present in the Doppler velocity log measurements is fully compensated by the bias terms of the filter.

B. MMAE

In this section a multi-model adaptive estimator based on a bank of multirate estimators previously presented will be briefly introduced [2]. The estimation problem was classically formulated as an hypothesis test associated with a state estimation problem. For that purpose a set of hypothesis $R = \{R_1, R_2, \ldots, R_K\}$ are considered, where the presence of the true model is assumed.

The MMAE estimator is derived from the set of white noise Gaussian random variables $\mathbf{r_i}(k) = y(k) - \mathbf{C}\hat{z}_\mathbf{i}(k)$, $r(k)$, corresponding to the Kalman filter residuals, with covariance $\mathbf{S_i}(k) = E[\mathbf{r_i}(k)\mathbf{r_i}(k)^T]$, $\mathbf{S_i}(k)$ computed as $\mathbf{S_i}(k) = \mathbf{C}(k)\mathbf{P_i^-}(k)\mathbf{C}(k)^T + R_\mathbf{i}(k)$. Based on the auxiliary scalar quantities $\beta_\mathbf{i}(k) = \frac{1}{(2\pi)^{m/2}\sqrt{det(\mathbf{S_i}(k))}}$ and $w_\mathbf{i}(k) = \mathbf{r_i}^T(k)\mathbf{S_i}^{-1}(k)\mathbf{r_i}(k)$, the hypothesis posterior probability can be updated using the recursion

$$p_\mathbf{i}(k) = \frac{\beta_\mathbf{i}(k)e^{-\frac{1}{2}w_\mathbf{i}(k)}}{\sum_{j=1}^{K}\beta_\mathbf{j}(k)e^{-\frac{1}{2}w_\mathbf{j}(k)}}p_\mathbf{i}(k-1), \tag{9}$$

where $p_\mathbf{i}(k)$ will be the weight for estimator i, to compute the posterior state estimate as $\hat{\mathbf{z}}_m(k) = \sum_{i=1}^{K} p_\mathbf{i}(k)\hat{\mathbf{z}}_\mathbf{i}(k)$, with a corresponding true posterior conditional covariance

$$\mathbf{P}_m(k) = \sum_{i=1}^{K} p_\mathbf{i}(k)\left(\mathbf{P_i^+}(k) + e(k)e(k)^T\right), \tag{10}$$

given the posterior error $e(k) = (\hat{\mathbf{z}}_\mathbf{i}(k) - \hat{\mathbf{z}}_m(k))$ for each estimator. In the case where the true model is present the corresponding weight will go to 1, in the linear time-invariant case. Otherwise, the weights of the models closer to the real one will have higher values, see [2], [6] for details.

V. Performance Assessment

The performance of the proposed PCA based positioning and MMAE navigation systems is assessed on a synthetic world, through extensive Monte Carlo simulations (based

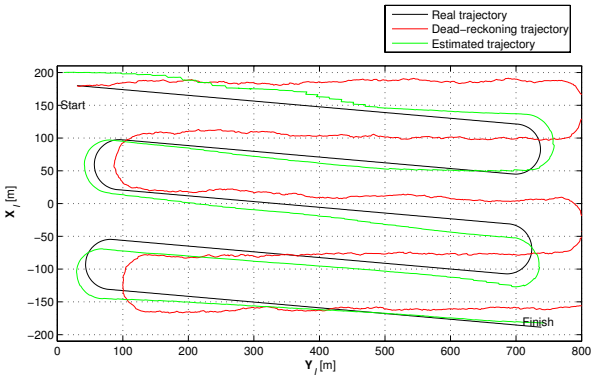

Fig. 6. Trajectory in the horizontal plane

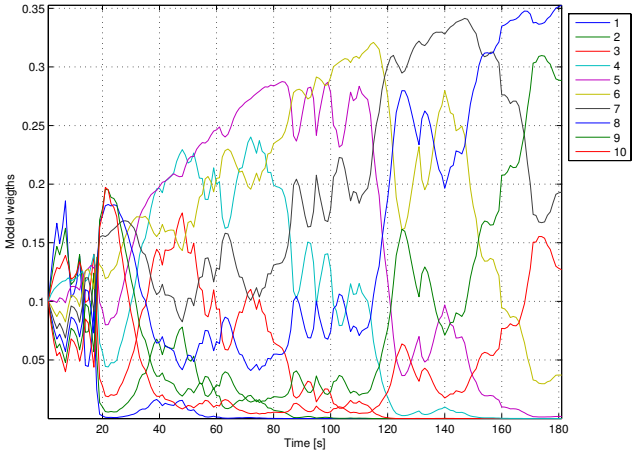

Fig. 7. Weights associated with the hypothesis models

TABLE I

SIMULATION PARAMETERS

Parameters	Values
Vehicle	
T, h	$1800\ s$, $1\ s$
${}^{\mathcal{B}}({}^{\mathcal{I}}\mathbf{v}_{\mathcal{B}})$	$[2\ 0\ 0]^T\ m\ s^{-1}$
$\mathbf{p}(0)$	$[30\ 180\ 50]^T\ m$
$\mathbf{b}$	$[0.1\ 0.2\ 0]^T\ m\ s^{-1}$
$\psi(0)$	$1.65\ rad$
Sensors	
$\sigma_{u,v}$	$6 \times 10^{-1}\ m\ s^{-1}$
$\sigma_{d(i)}$	$10^{-1}\ m$
σ_{ψ}	$pi/180\ rad$
PCA	
L, M	10, $42 * 25 = 1050$
$N = N_x * N_y$	$20 * 20$
n, δ	10, $80\ m$
Estimator	
$P_{\mathbf{i}}(0) = P(0)$	$diag(10^2\ 10^2\ 1\ 10^{-2}\ 10^{-2}\ 10^{-3})$
$Q_{\mathbf{i}} = Q$	$diag(10^{-3}\ 10^{-3}\ 10^{-3}\ 10^{-6}\ 10^{-6}\ 10^{-7})$
$\hat{\mathbf{p}}_{\mathbf{i}}(0) = \hat{\mathbf{p}}(0)$	$[10\ 200\ 10]^T\ m$
$\hat{\mathbf{b}}_{\mathbf{i}}(0) = \hat{\mathbf{b}}(0)$	$[0\ 0\ 0]^T\ m.sec^{-1}$
MMAE	
K	10
f^2	$[200\ 225\ 250\ 275\ 300\ 325\ 350\ 375\ 400\ 425]$

on 100 runs). The mission area is constrained to $x \in]-250, 250]\ m$, $y \in]0, 840]\ m$, and the terrain depth is given by

$$\begin{aligned} z(x,y) &= 80 + (-10sin(2\pi/400x)cos(2\pi/600y) \\ &- 20cos(2\pi/800x) + \eta_z) \left(\tfrac{x+250}{500}\right)^2, \end{aligned}$$

where η_z is correlated white noise. Note that along the x direction a fading factor is included, resulting in harder conditions for the feature based positioning system to operate. The set of parameters used are listed on table I as well as the initial parameters for the ideal vehicle and for the estimator. Note that the choice of δ can be critical: in the case of a large estimation error a small value can difficult to obtain the correct neighbor; the choice of a large δ augments the probability of misidentifying an incorrect neighbor.

The measurements of the simulated sensors are corrupted by white noise with characteristics similar to the sensors commercially available and commonly installed on UVs. The mission is composed by a sequence of trimming trajectories similar to the ones used in survey missions. In the first *leg*, in fig. 6, the estimation error is larger due to the initial position and bias estimate mismatches, to illustrate the performance of the estimator (depicted in figure 5). It is important to remark that along the mission the models recruited (as depicted in figure 7) correspond to higher values of f when the UV approaches the flatter terrain, adapting naturally to the terrain characteristics. These results validate the approach proposed on this paper. The advantages relative to the dead reckoning open loop integration can hardly be overemphasized.

VI. CONCLUSIONS AND FUTURE WORK

In this work tools for Terrain Based Navigation using a MMAE estimator, with a positioning sensor rooted on Principal Component Analysis are proposed, discussed in detail, and validated in simulation. However, the non-biased proposed positioning sensor presents nonlinear characteristics for different terrains and PCA parameters', that can be tackled resorting to multi-model adaptive estimation techniques.

The results obtained pave the way to the use of the proposed framework in navigation, guidance, and control applications of Autonomous Underwater Vehicles and Remotely Operated Vehicles, with the aim of impacting on overcoming the limitations that the UVs have today.

REFERENCES

[1] Alcocer, A., P. Oliveira and A. Pascoal (2004). Study and implementation of an EKF GIB-based underwater positioning system. *IFAC CAMS04*.

[2] Anderson, B. and Moore, J., *Optimal Filtering.* Prentice Hall, 1979. [5] M. Athans and C.

[3] Baker, W. and R. Clem. (1977). Terrain contour matching (tercom) primer. *ASD-TR-77-61, Aeronautical Systems Division, Wright-Patterson AFB*.

[4] Crowley, J., F. Wallner and B. Sciele (1998). Position estimation using principal components of range data. *Proceedings 1998 IEEE ICRA*.

[5] Fryxell, D., P. Oliveira, A. Pascoal, C. Silvestre and I. Kaminer (1996). Navigation, guidance and control systems of AUVs: An application to the MARIUS vehicle. *IFAC CEP*.

[6] Gelb, A. (1975). *Applied Optimal Estimation*. The M.I.T. Press.

[7] Hostetler, L. and R. Andreas (1983). Nonlinear kalman filtering techniques for terrain-aided navigation. *IEEE TAC, vol. AC-28, No. 3*.

[8] Jolliffe, I. (2002). *Pricipal Component Analysis*. Springer.

[9] Karlsson, R. and F. Gustafsson (2003). Particle filter for underwater terrain navigation. *2003 IEEE Workshop on Statistical Signal Processing*.

[10] Leonard, J., A. Bennett, C. Smith and H. Feder (1998). Autonomous underwater vehicle navigation. *MIT Marine Robotics Laboratory Technical Memorandum*.

[11] Mertins, A. (1999). *Signal Analysis: Wavelets, Filter Banks, Time-Frequency Transforms and Applications*. John Wiley & Sons.

[12] Nygren, I. and M. Jansson (2003). Robust terrain navigation with the correlation method for high position accuracy. *OCEANS 2003*.

[13] Oliveira, P. (2002). *Periodic and Nonlinear Estimators with Applications to the Navigation of Ocean Vehicles,* IST, UTL, Lisbon, Portugal.

[14] Oliveira, P. (2005). *Terrain Based Navigation Tools for Underwater Vehicles using Eigen Analysis,* 16^{th} IFAC World Congress, Prague.

[15] Oliveira P. (2005). PCA Positioning Sensor Characterization for Terrain Based Navigation of UVs, 2nd Iberian Conference on Pattern Recognition and Image Analysis, Estoril.

[16] Pham, D., K. Dahia and C. Musso (2003). A kalman-particle kernel filter and its application to terrain navigation. *Proceedings 6th ICIF*.

[17] Sistiaga, M., J. Opderbecke, M. Aldon and V. Rigaud (1998). Map based underwater navigation using a multibeam echosounder. *OCEANS 1998*.

[18] Vickery, K. (1998). Acoustic positioning systems - a pratical overview of current systems. *Proceedings of AUV'98*.

[19] Whitcomb, L., D. Yoerger and H. Singh (1999). Combined doppler/lbl based navigation of underwater vehicles. *11th International UUST99*.